Ahlem Chahinez Kadri[1], M'hamed Ouadah[1],
Abderrahmane Younes[2], Sofiane Chabane[3]*

[1]*Ecole Nationale Supérieure des Technologies Avancées, Place des Martyrs, 16001 Algiers, Algeria,* [2]*Research Center in Industrial Technologies (CRTI), Cheraga, Algiers, Algeria,* [3]*CIMA+, Montreal, Quebec, Canada*

Assessing the impact of AC, DC and hybrid AC/DC stray currents on cathodic protection efficiency

ABSTRACT

Ensuring the efficiency of cathodic protection (CP) is critical for maintaining the integrity of buried pipelines. Stray currents, particularly those originating from high-voltage power lines, can interfere with CP systems, leading to accelerated corrosion. This study investigates the effects of alternating current (AC), direct current (DC), and hybrid AC/DC stray currents on CP performance. Electrochemical measurements and finite element modeling (FEM) were employed to evaluate the impact of these currents on X70 steel pipelines. Results indicate that AC stray currents reduce CP effectiveness by shifting protection potentials to more electropositive values, increasing corrosion risk. DC stray currents affect CP voltage settings, while hybrid AC/DC interference exacerbates both effects. Findings provide insights into pipeline protection strategies, particularly in environments with mixed AC/DC stray currents.

Keywords: *AC stray current, DC stray current, hybrid AC/DC interference, corrosion, cathodic protection, finite element method (FEM)*

1. INTRODUCTION

Cathodic protection (CP) stands as one of the most commonly employed methods to safeguard pipelines against corrosion, either through impressed current anodes or by connecting them to sacrificial materials acting as anodes [1-5]. There are two primary types of CP systems(Fig.1): impressed current (ICCP) and sacrificial anode (SACP). In the ICCP system, an electrical current is supplied from an external source (rectifier), which is electrically connected between an anode and the pipeline cathode. Conversely, in the SACP system, the pipeline is electrically linked to the sacrificial anode.

Cathodic protection (CP) is widely used to mitigate pipeline corrosion, utilizing either impressed current cathodic protection (ICCP) or sacrificial anode cathodic protection (SACP) [1-5]. As shown in Figure 1, ICCP relies on an external power source to supply protective current, whereas SACP employs sacrificial materials that corrode in place of the pipeline.
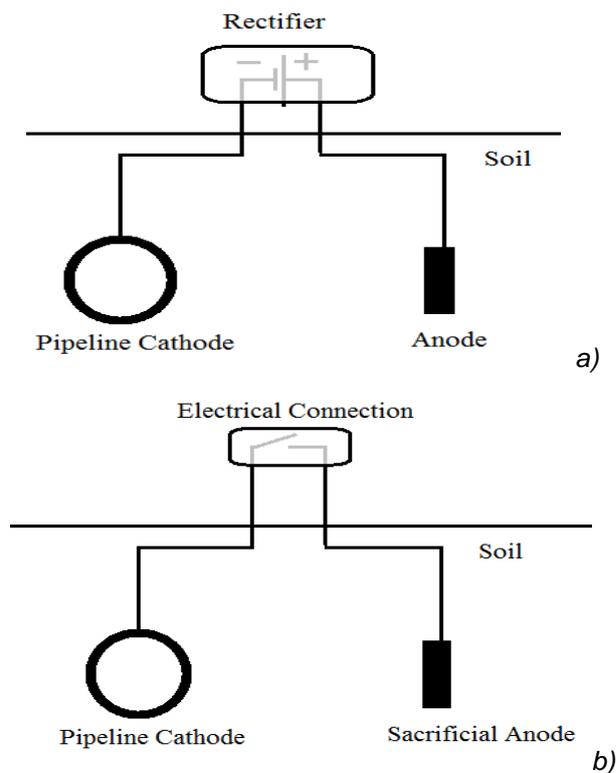

Figure 1. Cathodic protection system:
a) Impressed current cathodic protection,
b) Sacrificial anode cathodic protection

*Corresponding author: M'hamed Ouadah
E-mail: mhamed.ouadah@ensta.edu.dz

Stray currents can originate from either alternating current (AC) or direct current (DC), depending on their source [6,7]. For instance, AC stray currents may occur when alternating current flows through power line conductors, generating an electromagnetic field around these conductors. This field can couple with adjacent buried pipelines, inducing AC stray currents [8-15].

DC Stray currents can be categorized as either dynamic or static [16-17]. Dynamic stray currents are characterized by variations in amplitude and/or changes in the direction of current flow. These currents may originate from both manmade and natural sources. Manmade sources include DC welding equipment and DC electrical railway systems [18-23]. Telluric currents, on the other hand, are naturally occurring stray currents induced by disturbances in the Earth's magnetic field due to sunspot activity. In contrast, static stray currents maintain a constant amplitude and follow consistent geographical paths. Examples of static stray currents include high voltage direct current (HVDC) ground electrodes and cathodic protection systems.

Both AC and DC stray currents pose significant risks to buried steel pipelines, as they can cause corrosion and reduce the efficiency of cathodic protection [24-33]. In references [25] and [26], the impact of AC stray currents resulting from electromagnetic induction caused by high voltage power lines on cathodic protection performance (both sacrificial anode and impressed current cathodic protection) was investigated. The authors demonstrated that the protection potential becomes more electropositive with increasing AC stray current. This indicates that the likelihood of AC corrosion rises with higher induced AC stray currents, even when the pipeline is under cathodic protection. AC stray currents not only affect cathodic protection performance but also shift the applied cathodic protection potential on pipelines away from its intended design value.

This study presents a detailed assessment of the impact of AC, DC, and hybrid AC/DC stray currents on the cathodic protection (CP) performance of buried pipelines. By combining electrochemical measurements with finite element modeling (FEM), it quantifies how stray currents interfere with CP efficiency and contribute to corrosion acceleration in X70 steel pipelines. The findings offer valuable insights for enhancing pipeline protection strategies, particularly in areas influenced by high-voltage power lines.

To achieve this, a methodology was developed to evaluate the effects of stray currents on CP performance, utilizing electrochemical parameters obtained from experimental tests on X70 steel

pipelines. These parameters serve as boundary conditions in a cathodic protection model, ensuring a more accurate representation of real-world conditions.

The results demonstrate that as AC stray current density increases, the CP potential shifts in a more electropositive direction, reducing its protective effectiveness and heightening corrosion risk, even under CP. Additionally, the presence of a nearby pipeline further disturbs the CP potential of the protected pipeline, increasing its vulnerability to corrosion. Notably, at the intersection of two pipelines, when subjected to AC stray currents of 100 and 200 A/m², the second pipeline experiences a negative current density, causing stray currents to exit the pipeline. This phenomenon leads to a partial cathodic protection effect on the first pipeline, mitigating its corrosion risk.

This study enhances the understanding of stray current interference in CP systems and provides a foundation for developing mitigation strategies to improve pipeline longevity and reliability.

2. METHODOLOGY

This study focuses on diagnosing the effects of AC, DC, and combined AC/DC stray currents on cathodic protection (CP) performance. Electrochemical tests were conducted to determine X70 steel's response to stray currents. The study considered three scenarios: (1) a pipeline under AC stray current interference, (2) the impact of an intersecting pipeline on CP performance, and (3) the combined influence of AC and DC stray currents. Experimental polarization curves and electrochemical impedance spectroscopy (EIS) data were integrated into a finite element model to simulate real-world CP conditions.

The experimental setup included a three-electrode system with a saturated calomel electrode (SCE) as a reference, a platinum counter electrode, and an X70 steel working electrode. Stray current densities of 0 A/m², 100 A/m², and 200 A/m² were applied, and their effects on CP potential, corrosion rate, and polarization behavior were analyzed.

This study focuses on diagnosing the effects of AC, DC, and combined AC/DC stray currents on cathodic protection (CP) performance. The methodology relies on electrochemical measurements to determine the electrochemical parameters of X70 steel pipelines. Stray current densities of 0 A/m², 100 A/m², and 200 A/m² were applied to the X70 steel using two electrodes connected to an AC stray current source as presented in Fig.2. This allowed for the extraction of polarization corrosion parameters (such as Tafel slopes, corrosion current densities, and corrosion

potentials) under various AC stray current densities. These parameters serve as boundary conditions in a Finite Elements Method (FEM) cathodic protection model. To assess the effects of AC, DC, and combined AC/DC stray currents on CP performance, we examined two intersecting pipelines at a 90° angle. Pipeline n°1 is protected from corrosion by an impressed current cathodic protection system, while Pipeline n°2 intersects Pipeline n°1 without applied cathodic protection. Three Scenarios were developed:

Scenario 01: The first case involves only Pipeline n1 under the influence of AC stray current (Fig. 3).

Scenario 02: the pipeline n°1 without the influence of AC stray current intersecting Pipeline n2 (Fig. 4).

Scenario 03: Combines the effects of both scenarios (Figure 5).

The pipelines, measuring 40m in length, have an outside radius of 210 mm and a wall thickness of 10 mm.
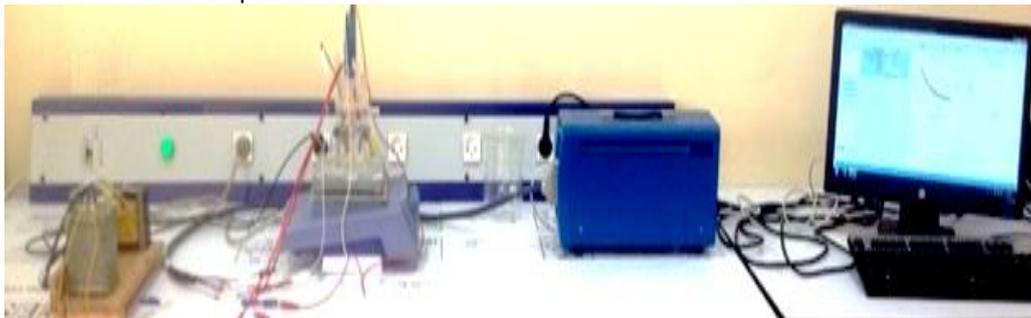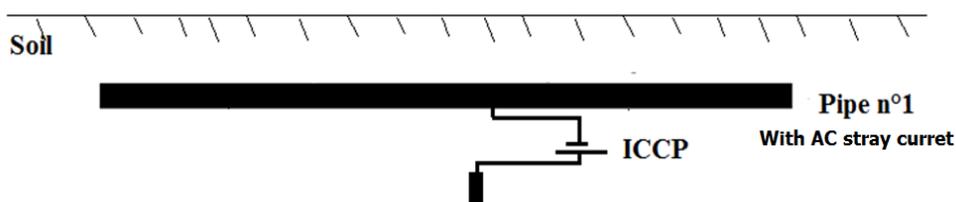

Figure 2. Electrochemical test bench

Figure 3. The Schematic representation of the system used to identify the impact of AC stray current on the cathodic protection performance
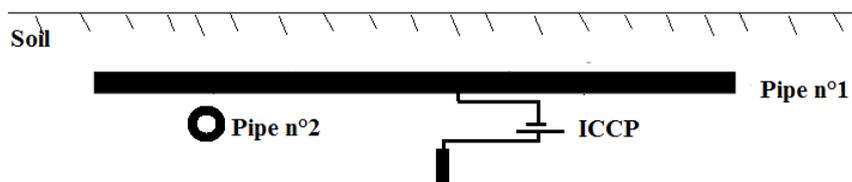

Figure 4.The Schematic representation of the system used to identify the impact of DC on the cathodic protection performance

Figure 5. Schematic representation of the system employed to assess the influence of combined AC and DC stray currents on cathodic protection performance

2.1. Cathodic Protection Model

The fundamental components of the cathodic protection system include: the anode (Γ_1), the cathode (Γ_2), and the electrolyte (Ω). Designing the CP system necessitates solving Laplace's equation $\nabla^2 V = 0$ with appropriate boundary conditions to determine the potential and current density distribution within the solution domain. Figure 6 illustrates the various boundary conditions utilized based on the nature of the boundary.
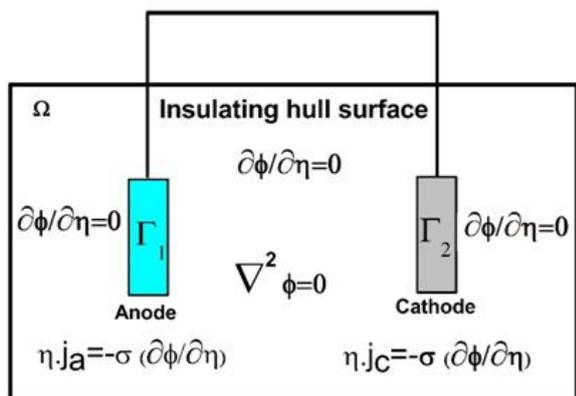
Figure 6. Principle of the cathodic protection system boundary conditions: $\Gamma 1$ is the anode, $\Gamma 2$ is the cathode and Ω is the electrolyte

For symmetry boundaries, the following boundary condition was applied:

$$\frac{\partial V}{\partial n} = n.\nabla V = 0 \tag{1}$$

Where V represents the electrical potential and n denotes the normal to the boundary surface.

- Along the anode, the CP system imposes an output current regulated by a rectifier. The current flowing out of the anode surface is uniform. Therefore, the anode boundary condition can be expressed as follows:

$$I = I_{anode} = 0 \tag{2}$$

- Along the pipeline surface, the utilized boundary condition is as follows:

$$n.J_c = -\sigma \frac{\partial V}{\partial n} = f_c(V) \tag{3}$$

Where $f_c(V)$ represents the electrochemical relationship between the current densities (J_c) and the potentials (V). This relationship is depicted by nonlinear curves, referred to as polarization curves, obtained through electrochemical measurements.

2.1. Materials and experimental procedures

In this study, the X70 steel pipeline was utilized. The XRD pattern depicted in Figure 7 typically reveals peaks corresponding to the ferrite (α-Fe) phase, the primary constituent of X70 steel, with small amounts of pearlite potentially present depending on the composition and processing conditions.

The sharpness and intensity of the peaks provide insights into the material's crystallinity and residual stress levels, both critical for pipeline applications, where high crystallinity and minimized residual stress are essential to ensure mechanical reliability.

The microstructure of the X70 steel matrix, illustrated in Figure 8, predominantly features a ferritic-pearlitic structure, where ferrite imparts ductility, and pearlite enhances strength.

A refined grain structure is vital for optimizing the steel's strength and toughness, especially in demanding low-temperature conditions. Further more, reducing non-metallic inclusions through advanced steelmaking techniques is crucial to enhancing weldability and minimizing the likelihood of fractures, thereby ensuring superior performance and reliability in pipeline applications.
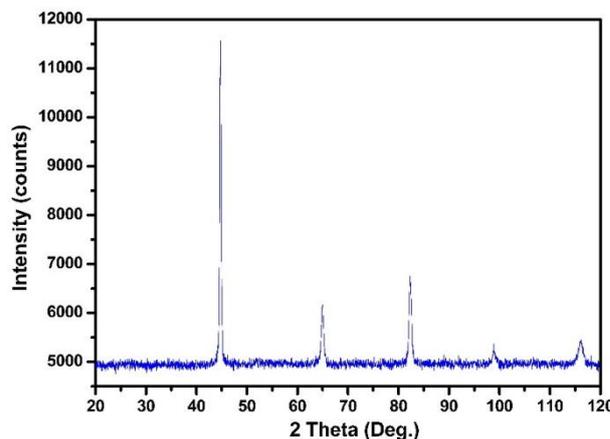

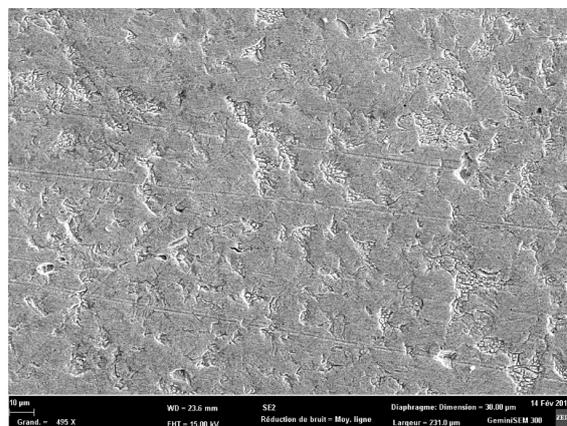*Figure 7. An X-ray diffraction (XRD) analysis of the X70 steel.*

Figure 8. Microstructure of X70 pipeline steel

Electrochemical measurements were conducted using a Bio-Logic SP-150 electrochemical workstation controlled by a PC. A three-electrode system was employed: TheX70 steel specimen served as the working electrode (WE), a saturated calomel electrode (SCE) was utilized as the reference electrode (RE), and a platinum wire acted as the counter electrode (CE). The electrolyte utilized in this investigation was a simulated soil solution, consisting of MgSO4·7H$_2$O (0.131g), CaCl$_2$·2H$_2$O (0.18g), KCl (0.122g), and NaCO$_3$ (0.483g) [34].

Electrochemical Impedance Spectroscopy (EIS) is an effective technique for evaluating the

corrosion resistance of X70 steel in simulated soil solution affected by AC interference. Figures 9-12 show the Nyquist plots and bode plots of X70 steel in simulated soil solutions at different AC densities. The electrochemical impedance spectroscopy data were fitted using the equivalent circuit shown in Fig. 12, where a constant phase element, C, represents a double-layer capacitor, R1 represents the solution resistance, and R2 denotes the double-layer resistance. The fitting results are listed in Table 1, indicating that as the AC current density increased, R2 decreased, suggesting a reduction in the corrosion resistance of X70 steel. This indicates that the corrosion rate increased with higher AC current density values. Also, it can be seen that the diameter of the capacitive loop gradually decreased with increasing AC current density, indicating that the AC corrosion rate increased with increasing AC current density.

Bode plot analysis shows that at low frequencies the impedance amplitude is lower, suggesting a more active corrosion process. Under the influence of AC interference, this amplitude generally decreases, indicating reduced corrosion resistance. Also, it can be seen from the phase angle that the decrease in phase angle in the low-frequency region suggests increased corrosion activity, as the system becomes more resistive and less capacitive.
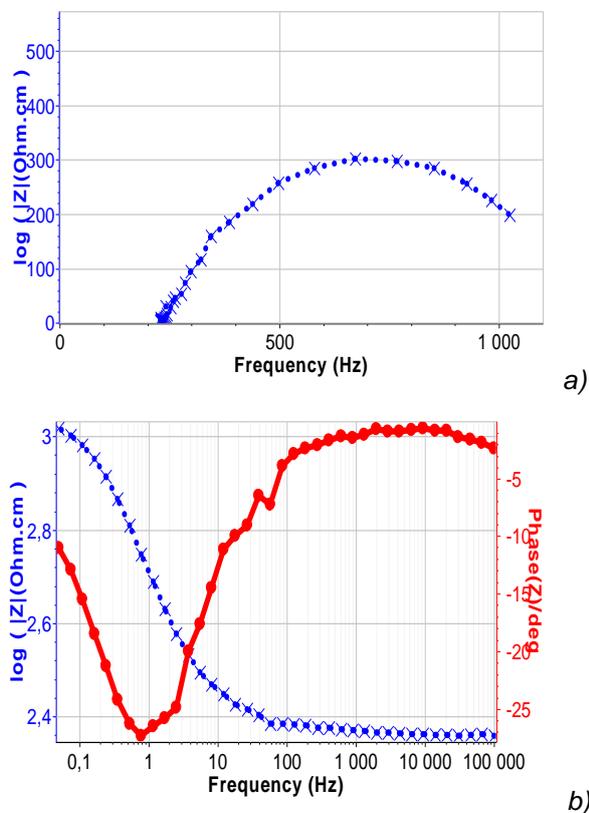

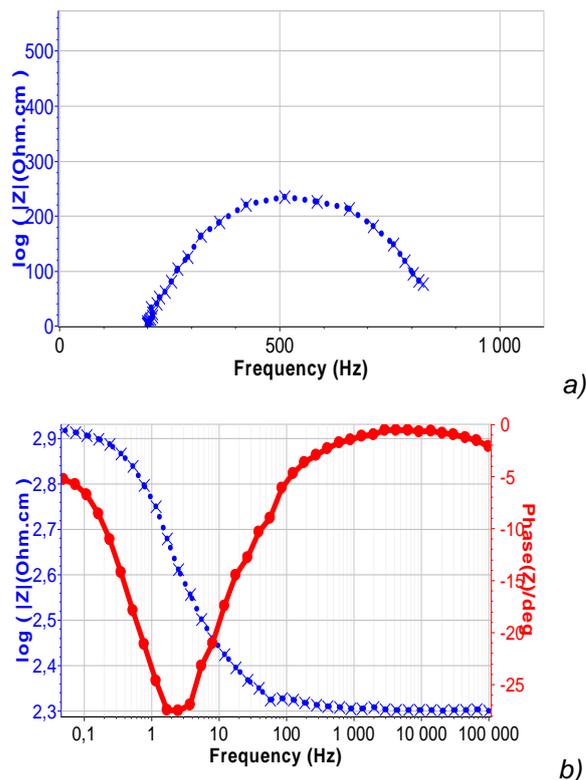*Figure 10. Nyquist plots (a) and Bode plots (b) of X70 steel in simulated soil solutions under a current density of 100 A/m²*

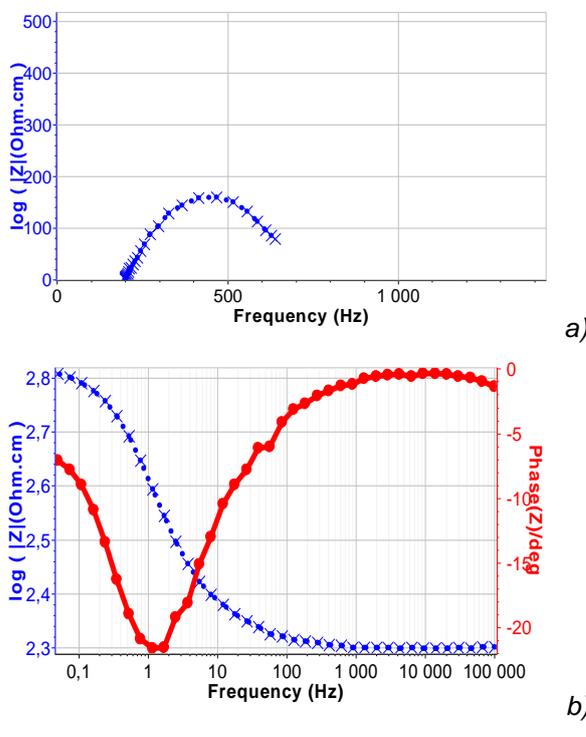*Figure 9. Nyquist plots (a) and Bode plots (b) of X70 steel in simulated soil solutions*

Figure 11. Nyquist plots (a) and Bode plots (b) of X70 steel in simulated soil solutions under a current density of 200 A/m²
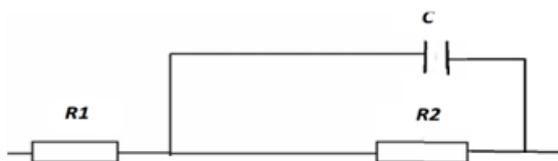
Figure 12. Equivalent circuit diagram

Table 1. Fitting results of EIS data of X70 steel in simulated soil solution under No AC current density, 100 A/m² and 200 A/m²

AC current density	R1(Ωcm)	C(F)	R2(Ωcm)
No AC current density	201,8	44,84e-9	1001,1
With 100 A/m²	201,3	63,07e-6	653,5
With 200 A/m²	199,7	67,48e-6	485,8

Figute 13 illustrates the polarization curve of X70 steel in the simulated soil solution under various AC stray current densities. The results derived from fitting the polarization curves shown in Figure 13 are summarized in Table 2, presenting the corrosion current density (Icorr), corrosion potential (Ecorr), and Tafel slopes (b_{anodic}, $b_{cathodic}$).

The polarization curves reveal a clear trend of increased corrosion activity with rising AC interference. As the AC stray current density increases from 0 to 200 A/m², the corrosion potential (Ecorr) shifts positively from -769.39 mV.SCE to -710.26 mV.SCE, indicating a higher electrochemical reactivity of the steel surface. Simultaneously, the corrosion current density (Icorr) rises significantly from 12.64 µA/cm² at 0 A/m² to 46.36 µA/cm² at 200 A/m², demonstrating that AC stray currents accelerate the corrosion process. The anodic Tafel slope (ba) increases slightly, while the cathodicTafel slope (bc) shows a sharp rise, suggesting that AC stray currents primarily influence the cathodic reaction, potentially altering oxygen reduction kinetics. These findings indicate that AC stray currents not only enhance the overall corrosion rate but also modify electrochemical behavior, with significant implications for cathodic protection strategies in AC-interfered environments.
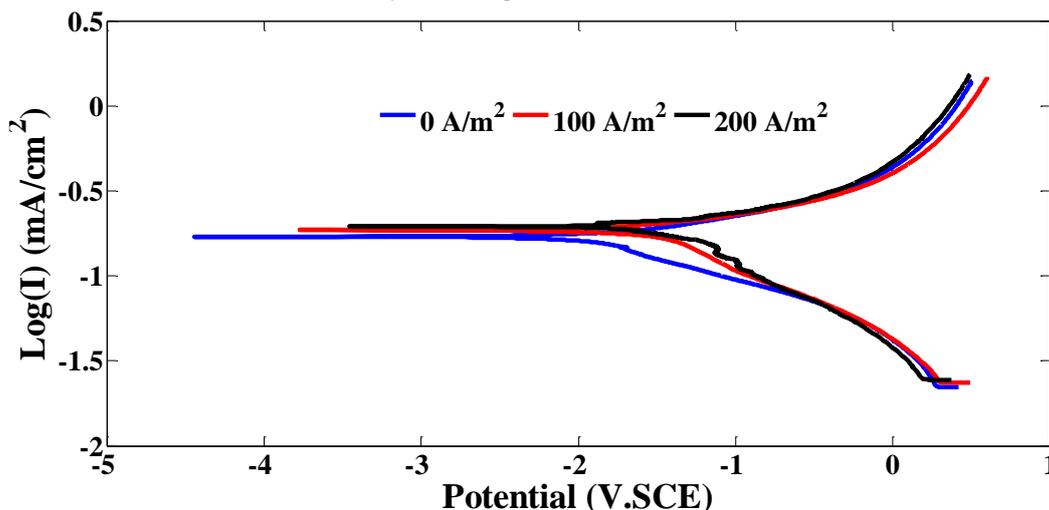

Figure 13. Polarization curves of X70 steel under various AC stray current densities

Table 2. Tafel slopes, corrosion current densities, and corrosion potentials obtained from polarization curves under various AC stray current densities

AC stray current density, (A/m²)	ba (mV)	bc (mV)	Icorr (µA/cm²)	Ecorr (mV.SCE)
0	173.1	247.1	12.64	-769.39
100	175.5	466.3	31.41	-731.39
200	204.0	671.6	46.36	-710.26

3. RESULTS AND DISCUSSION

3.1. Scenario 01:AC Stray Current Effects on CP Performance

To investigate the impact of AC stray current on cathodic protection performance, the scenario depicted in Fig. 3 was considered. The simulation model comprises the following elements: pipeline n°1 protected from corrosion by an impressed current cathodic protection system, with an anode output current of 4 A. Pipeline n°1 is subjected to AC stray current densities of 0 A/m2, 100 A/m², and 200 A/m².

For the 4 A output current, Figure 14 illustrates the distribution of CP potential along the pipeline under the influence of AC stray current densities of 0, 100, and 200 A/m^2. It is evident from this figure that, in the absence of stray current (0 A/m^2), the CP potential ranges between -1.37 V and -0.81 V vs. SCE, with the surface area facing the anode exhibiting the lowest value of -1.37 V vs. SCE. According to references [35, 36], the recommended effective cathodic protection potential (E-protection) for buried steel pipelines is less than -0.780 V vs.

SCE. Therefore, for an output current of 4 A, the pipeline is fully protected against corrosion.

Furthermore, it can be observed from this figure that induced AC stray current densities cause a deviation of the cathodic protection potential from its design value. The CP potential becomes more positive with increasing AC stray current densities. This indicates that the likelihood of corrosion increases with higher AC stray current densities, even when the pipeline is under cathodic protection.
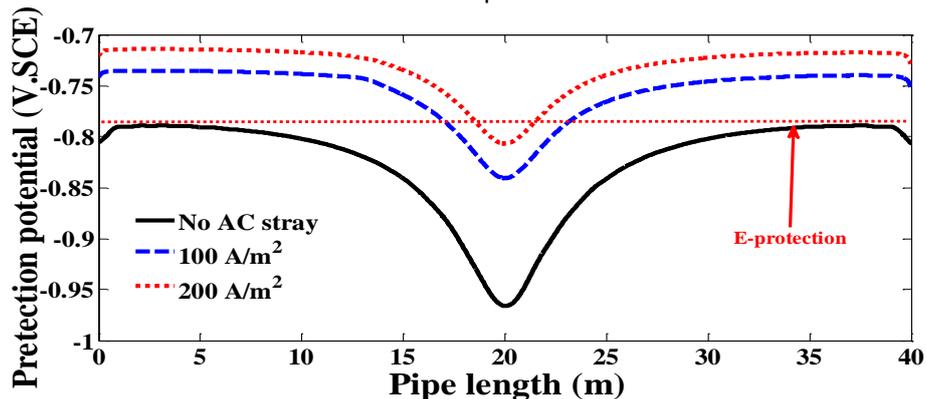

Figure 14. Effects of the AC stray current densities on the CP performance

3.2. Scenario 02:DC Stray Current Effects on CP Performance

Considering the scenario of two intersecting pipelines (Pipeline n°1 and Pipeline n°2) as illustrated in Fig.4, the simulation model comprises the following elements: Pipeline n°1 is protected from corrosion by an impressed current cathodic protection system, with an anode output current of 4 A. Pipeline n°2 intersects pipeline n°1 but does not have any applied cathodic protection.

Figure 15 illustrates the distribution of cathodic protection potential along pipeline n°1 concerning

pipe length, both with and without the presence of pipeline n°2. In the absence of pipeline n°2, pipeline n°1 exhibits full protection against corrosion. However, the introduction of pipeline n°2 significantly alters the cathodic protection potential of pipeline n°1, particularly at the intersection point, where a noticeable increase in potential occurs. This shift indicates that the presence of pipeline n°2 disrupts the cathodic protection potential of pipeline n°1 from its intended design, consequently increasing the probability of corrosion despite being under cathodic protection.
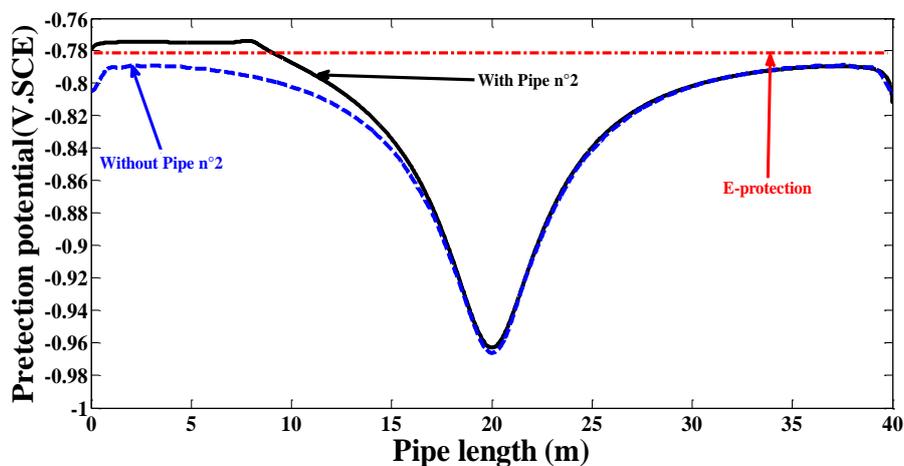

Figute 15. Cathodic protection potential distribution along pipelinen°1 as a function of pipe length with and without the presence of pipelinen°2

Figure 16 depicts the distribution of cathodic protection current density along the pipeline n°1 with respect to pipe length. Near the intersection, the protection current density diminishes, reaching nearly zero at the point of intersection between the two pipelines. Consequently, the effectiveness of pipeline cathodic protection is compromised around the intersection, resulting in inadequacy.
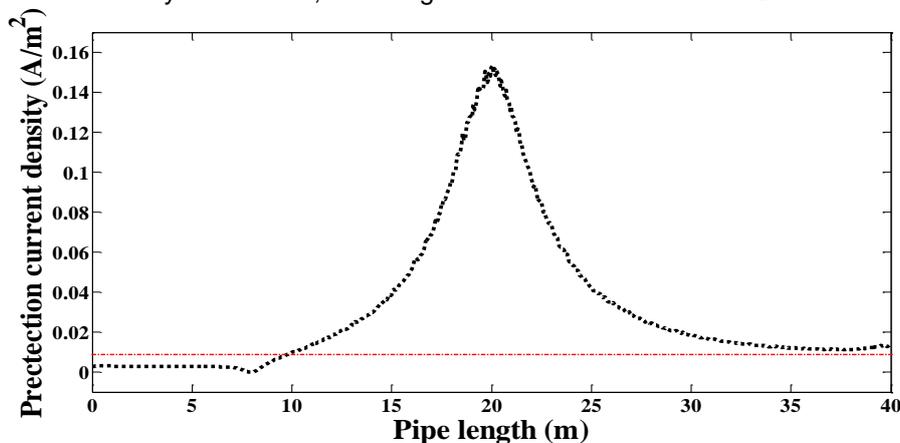

Figure 16. Cathodic protection current density distribution along pipelinen°1 as a function of pipe length

Figures 17 and 18 portray the potential and stray current density distributions along Pipeline n°2 concerning pipelinelengths, respectively. Notably, significant changes in potential distribution are observed at the intersection of the two pipelines, indicating the substantial impact of the intersection. Moreover, the stray current density is nearly negligible at the intersection point between the two pipelines.
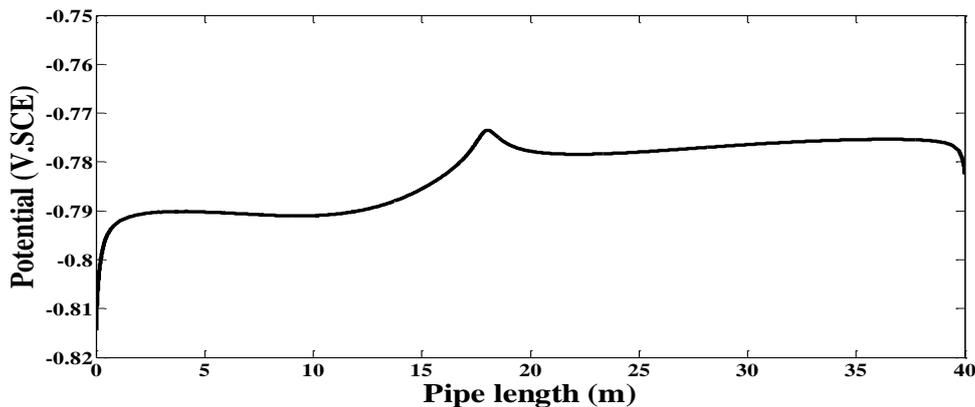

Figure 17. Potential distribution along pipelinen°2 as a function pipe length
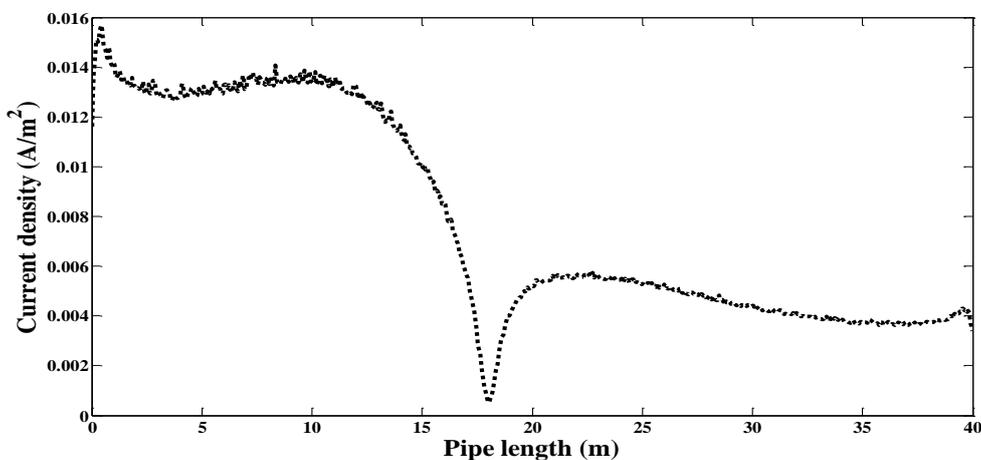

Figure 18. Stray current density distribution along pipelinen°2 as a function pipe length

3.3. Scenario 03: Hybrid AC/DC Stray Current Effects

In the preceding sections of this paper, we examined the impact of AC and DC stray currents on cathodic protection performance. Now, we delve into the effects of combined AC/DC stray currents on cathodic protection efficacy. We consider the scenario of two intersecting pipelines (pipeline n°1 and pipelinen°2), as illustrated in Fig. 5.

The simulation model comprises the following: Pipe n1 is shielded from corrosion by an impressed current cathodic protection system with an anode output current of 4 A. Pipelinen° 1is subjected to AC stray current densities of 0, 100 A/m², and 200 A/m2. Pipelinen°2 intersects pipelinen°1 but lacks cathodic protection.

Figures 19 and 20 depict the distributions of cathodic protection potential and current density along pipelinen°1 concerning pipe length under the influence of AC stray current densities of 0, 100, and 200 A/m², with the presence of pipelinen°2. The cathodic protection potential becomes more positive with increasing AC stray current. At the intersection of the two pipelines and for AC stray current densities of 100 and 200 A/m², we observe that as the AC stray current densities increase, the protection potential of pipelinen°1 becomes more negative, accompanied by an increase in protection current density. This indicates that pipelinen°1 receives some cathodic protection, mitigating corrosion.
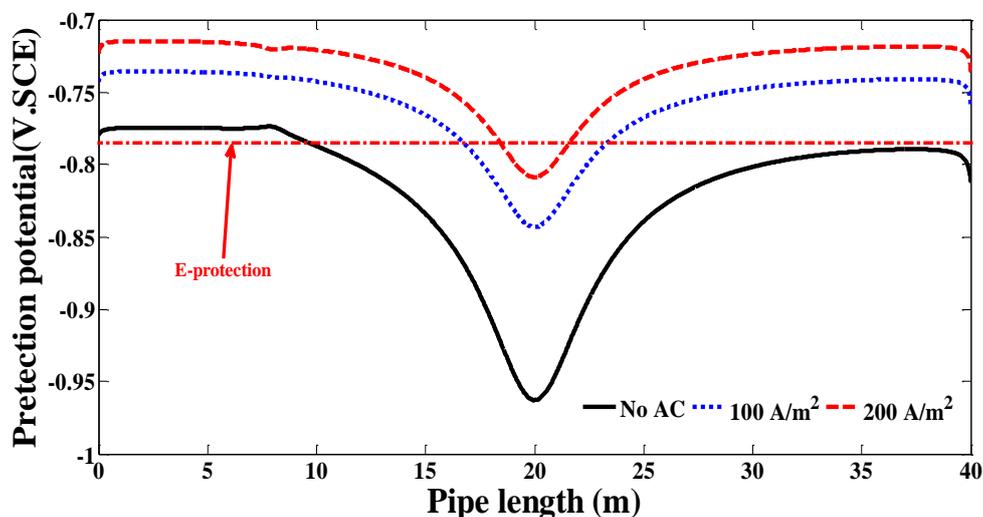

Figure 19. Distribution of cathodic protection potential along pipeline n°1 as a function of pipe length, considering the influence of AC stray current densities of 0, 100 A/m², and 200 A/m² in the presence of pipeline n°2
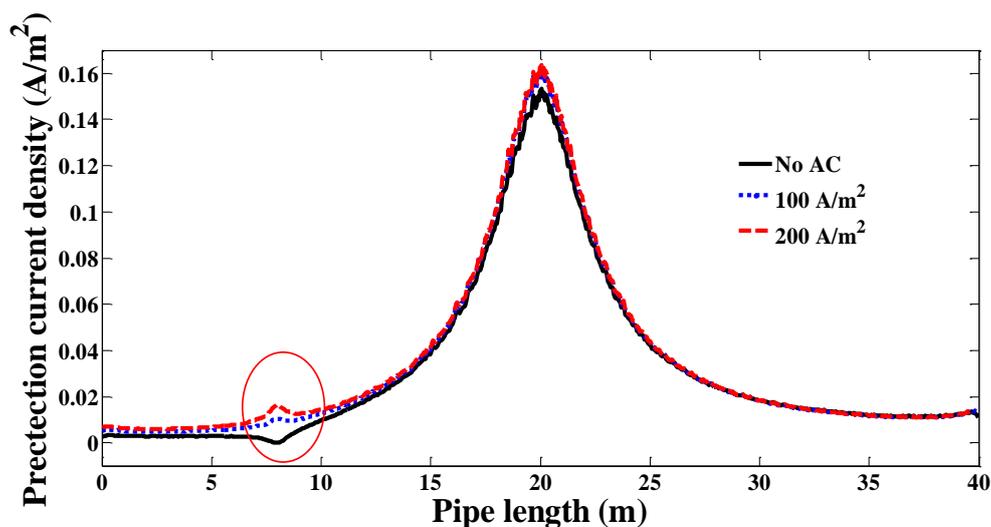

Figure 20. Distribution of cathodic protection current density along pipeline n°1 as a function of pipe length, considering the influence of AC stray current densities of 0, 100 A/m², and 200 A/m2 in the presence of pipeline n°2

Figures 21 and 22 illustrate the distributions of stray current density and potential along Pipe n°2 concerning pipe length for AC stray current densities of 0, 100, and 200 A/m², respectively. At the intersection of the two pipelines and for AC stray current densities of 100 and 200 A/m², the stray current density of pipelinen°2 is negative, signifying that the stray current flows out of pipelinen°2. Consequently, that section of the pipeline acts as an anode, with its potential higher than the corrosion potential of the X70steel , exacerbating corrosion on pipelinen°2.
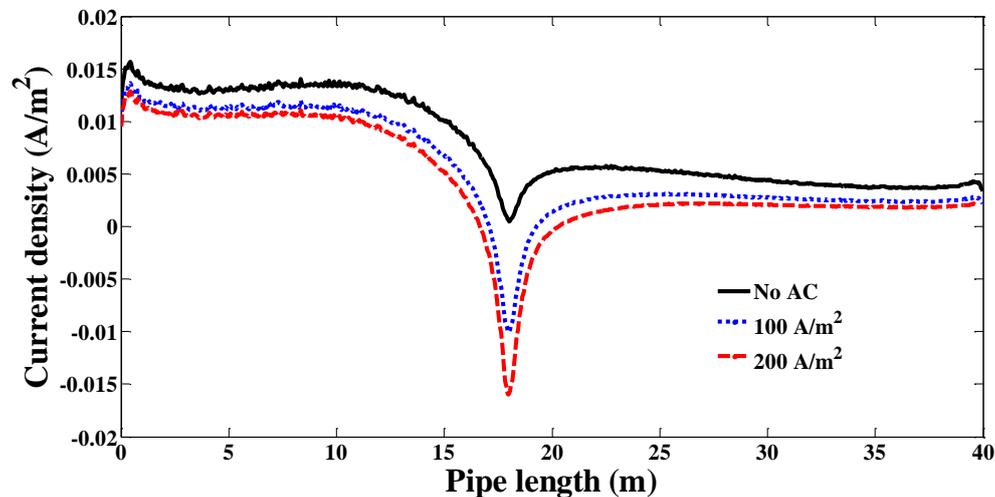

Figute 21. Stray current density distribution along pipelinen°2 as a function of pipe length for AC stray current densities of 0, 100 A/m² and 200 A/m²
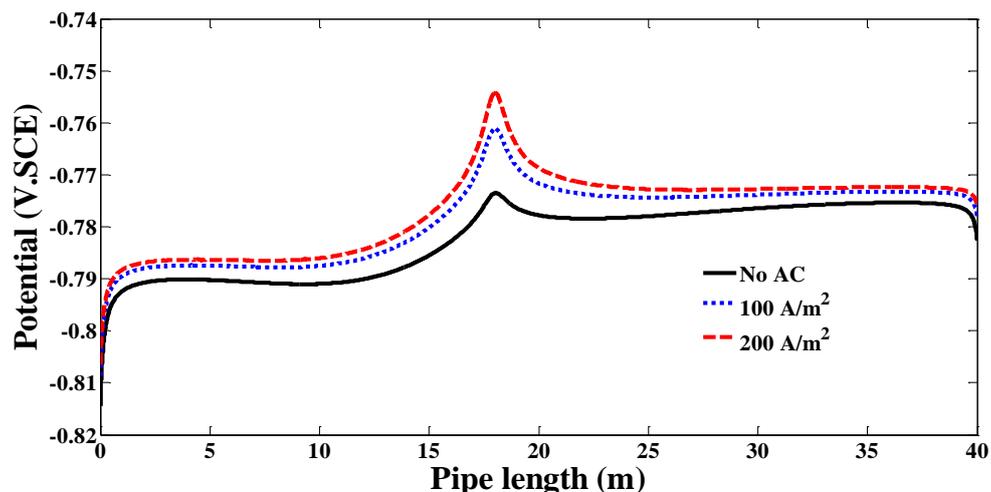

Figure 22. Potential distributions along pipelinen°2as a function of pipe length for of AC stray current densities of 0, 100 A/m² and 200 A/m²

4. CONCLUSION

In this paper, we investigated the effects of AC, DC, and combined AC/DC stray currents on the cathodic protection (CP) performance of the X70 steel pipeline. Our findings reveal several important insights:

- The likelihood of corrosion increases with higher AC stray current densities, even when the pipeline is under cathodic protection.
- The presence of pipeline n°2 significantly impacts the cathodic protection potential of pipeline n° 1 at their intersection.
- Pipelinen°2's presence shifts the cathodic protection potential of pipeline n°1 away from its design values.
- The presence of pipeline n°2 increases the risk of corrosion for pipeline n°1, even with cathodic protection applied.
- At the intersection of the two pipelines and for AC stray current densities of 100 and 200 A/m², pipeline n°1's protection potential becomes more negative, and the protection current density increases.

- Sections of pipeline n°1 experiencing increased current density receive some level of cathodic protection, reducing corrosion.
- At the intersection of the two pipelines and for AC stray current densities of 100 and 200 A/m², pipeline n°2 exhibits negative current density, indicating stray current flow out of the pipeline.

5. REFERENCES

[1] D.Lauria,M.Pagano,C.Petrarca,C.Pisani (2015) A novel approach to design cathodic protection system for high-voltage transmission cables,IEEE Trans.Ind.Appl.,51(6),5415–5420.
https://doi.org/10.1109/TIA.2015.2411735

[2] H.M.H.Farh, M.E.A.B.Seghier, T.Zayed (2023) A comprehensive review of corrosion protection and control techniques for metallic pipelines, Eng. Fail. Anal., 143, 106885.
https://doi.org/10.1016/j.engfailanal.2022.106885

[3] D.Lauria,S.Minucci,F.Mottola,M.Pagano,C.Petrarca (2018) Active cathodic protection for HV power cables in undersea application,Electr. Power Syst.Res.,163,590–598.
https://doi.org/10.1016/j.epsr.2017.11.016

[4] C.Christodoulou,G.Glass,J.Webb,S.Austin,C.Goodier (2010) Assessing the long term benefits of impressed current cathodic protection, Corros. Sci.,52(8),2671 2679.
https://doi.org/10.1016/j.corsci.2010.04.018

[5] I.D. Kim, E. C. Nho (2005) Module-type switching rectifier for cathodic protection of underground and maritime metallic structures, IEEE Trans.Ind. Electron., 52(1),181–189.
https://doi.org/10.1109/TIE.2004.841094

[6] X.H.Wang et al. (2013) Study on AC stray current corrosion law of buried steel pipelines, Appl. Mech.Mater.,263–266,448–451.

[7] D.Paul (2016) DC stray current in rail transit systems and cathodic protection [History],IEEEInd.Appl. Mag., 22(1),8 13.
https://doi.org/10.1109/MIAS.2015.2481754.

[8] H.Zhang,G.Karady,J.Hunt (2011) Effect of various parameters on the inductive voltage and current on pipelines, IEEE PES General Meeting, 17.
https://doi.org/10.1109/PES.2011.6038882.

[9] G.Lucca (2018) Different approaches in calculating AC inductive interference from power lines on pipelines,IET Sci. Meas.Technol.,12(6),802–806.
https://doi.org/10.1049/iet-smt.2018.0086

[10] K.B. Adedeji (2016) Effect of HVTL phase transposition on pipelines induced voltage, IJEEI, 4(2), 93–101.
https://doi.org/10.52549/ijeei.v4i2.209

[11] A.Popoli, A.Cristofolini, L.Sandrolini (2021) A numerical model for the calculation of electromagnetic interference from power lines on nonparallel underground pipelines, Math. Comput. Simul., 183,221–233.
https://doi.org/10.1016/j.matcom.2020.02.015

[12] L.Qi,H. Yuan, Y.Wu, X.Cui (2013) Calculation of overvoltage on nearby underground metal pipeline due to lightning strike on UHV AC line tower, Electr. Power Syst.Res.,94,54–63.
https://doi.org/10.1016/j.epsr.2012.06.011

[13] D.Micu, G.Christoforidis, L.Czumbil (2013) AC interference on pipelines due to double circuit power lines: A detailed study,Electr.Power Syst. Res., 103, 1–8.
https://doi.org/10.1016/j.epsr.2013.04.008

[14] F.Dawalibi (1986) Electromagnetic fields generated by overhead and buried short conductors.Part 1 - Single conductor,IEEE Trans.Power Deliv., 1(4), 105–111.
https://doi.org/10.1109/TPWRD.1986.4308036

[15] K.B.Adedeji et al. (2018) AC induced corrosion assessment of buried pipelines near HVTLs: A case study of South Africa, PIER B.
https://doi.org/10.2528/PIERB18040503

[16] C.A.Charalambous, P.Aylott (2014) Dynamic stray current evaluations on cut-and-cover sections of DC metro systems,IEEE Trans. Veh. Technol., 63(8), 3530–3538.
https://doi.org/10.1109/TVT.2014.2304522

[17] M.Ormellese, S.Beretta, F.Brugnetti, A.Brenna (2021) Effects of non-stationary stray current on carbon steel buried pipelines under cathodic protection, Constr.Build.Mater.,281,122645.
https://doi.org/10.1016/j.conbuildmat.2021.122645

[18] G.Cui, Z.L.Li, C.Yang, M.Wang (2016) The influence of DC stray current on pipeline corrosion, Pet.Sci., 13, 135–145.
https://doi.org/10.1007/s12182-015-0064-3

[19] A.Dolara, F.Foiadelli, S.Leva (2012) Stray current effects mitigation in subway tunnels,IEEE Trans. Power Deliv.,27(4),2304–2311.

[20] A.Ogunsola, L.Sandrolini, A.Mariscotti (2015) Evaluation of stray current from a DC-electrified railway with integrated electric–electromechanical modeling and traffic simulation,IEEE Trans.Ind.Appl.,51(6),5431–5441.

[21] J.V.Rodriguez, J.S.Feito (2013) Calculation of remote effects of stray currents on rail voltages in DC railway systems,IETElectr.Syst.Transp., 3(2),31–40.

[22] S.Aatif,H.Hu,F.Rafiq,Z.He(2021)Analysis of rail potential and stray current in MVDC railway electrification system,Railw.Eng.Sci.,29,394–407.
https://doi.org/10.1007/s40534-021-00243-0

[23] S.Lin, Q.Zhou, X.Lin, M.Liu, A.Wang (2020) Infinitesimal method based calculation of metro stray current in multiple power supply sections,IEEE Access, 8, 96581–96591.
https://doi.org/10.1109/ACCESS.2020.2994125

[24] A.Brenna,S.Beretta,F.Bolzoni,M.Pedeferri,M.Ormellese (2017) Effects of AC-interference on chloride-induced corrosion of reinforced concrete, Constr. Build. Mater.,137,76-84.
https://doi.org/10.1016/j.conbuildmat.2017.01.087

[25] M.Ouadah,O.Touhami,R.Ibtiouen (2016) Diagnosis of the AC current densities effect on the cathodic

protection performance of steel X70 for a buried pipeline due to EMI caused by HVPTL, Prog. Electromagn. Res.M.,45,163–171.

[26] M.Ouadah, O.Touhami, R.Ibtiouen (2017) Method for diagnosis of the effect of AC on the X70 pipeline due to inductive coupling caused by HVPL, IETSci. Meas. Technol.,11(6),766–772. https://doi.org/10.1049/iet-smt.2016.0519

[27] D.Kuang, Y.F.Cheng (2017) Effects of AC interference on cathodic protection potential and its effectiveness for corrosion protection of pipelines, Corros.Eng.Sci.Technol.,52(1),22–28. https://doi.org/10.1080/1478422X.2016.1175773

[28] A.K.Thakur, A.K.Arya, P.Sharma (2020) The science of AC-induced corrosion: A review of pipeline corrosion due to HV AC lines, Corros. Rev., 38(6), 463–472. https://doi.org/10.1515/corrrev-2020-0044

[29] M.Ouadah, O.Touhami, R.Ibtiouen, A.Bouzida (2019) Diagnoses and mitigation of corrosion due to EMI between HVPTL and buried pipeline,IEEE CAGRE.https://doi.org/10.1109/CAGRE.2019.8713 291

[30] C.Wen, J.Li, S.Wang, Y.Yang (2015) Experimental study on stray current corrosion of coated pipeline steel,J.Nat.Gas Sci.Eng.,27(3),1555–1561.

[31] S.A. Memon, P. Fromme (2014) Stray current corrosion and mitigation in DC transit systems,IEEE Electr.Mag.,2(3),22–31.

[32] M.Ouadah, O.Touhami, R.Ibtiouen, M. F. Belmnaouar, M.Zergoug (2017) Corrosive effects of electromagnetic induction caused by HVPL on buried pipelines,Int.J.Electr.Power Energy Syst., 91 (2), 34–41. DOI:10.1016/j.ijepes.2017.03.005

[33] M.Ouadah, O.Touhami, R.Ibtiouen (2016) Diagnosis of AC corrosion on buried pipeline due to HV power line,J.Electr.Eng.,16(2),76–83.

[34] R.N.Parkins, W.K.Blanchard, B.S.Delanty (1994) Transgranular SCC of high-pressure pipelines in near-neutral pH,Corrosion,50(5),394–408.

[35] H.H.Uhlig, R.W.Revie (1985) Corrosion and corrosion control,John Wiley,New York.

[36] D.M.Kaufman (2003) Applying educational theory in practice,BMJ,326(7382),213–216. https://doi.org/10.1136/bmj.326.7382.213

IZVOD

PROCENA UTICAJA AC, DC I HIBRIDNIH AC/DC LUTAJUĆIH STRUJA NA EFIKASNOST KATODNE ZAŠTITE

Obezbeđivanje efikasnosti katodne zaštite (KZ) je ključno za održavanje integriteta zakopanih cevovoda. Lutajuće struje, posebno one koje potiču iz visokonaponskih dalekovoda, mogu ometati KP sisteme, što dovodi do ubrzane korozije. Ova studija istražuje efekte naizmenične struje (AC), jednosmerne struje (DC) i hibridnih AC/DC lutajućih struja na performanse KZ. Elektrohemijska merenja i modeliranje konačnih elemenata (FEM) korišćeni su za procenu uticaja ovih struja na čelične cevovode X70. Rezultati pokazuju da AC lutajuće struje smanjuju efikasnost KZ pomeranjem potencijala zaštite na elektropozitivnije vrednosti, povećavajući rizik od korozije. DC lutajuće struje utiču na podešavanja napona KZ, dok hibridna AC/DC interferencija pogoršava oba efekta. Rezultati pružaju uvid u strategije zaštite cevovoda, posebno u okruženjima sa mešovitim AC/DC lutajućim strujama.
Ključne reči: *AC lutajuća struja, DC lutajuća struja, hibridna AC/DC interferencija, korozija, katodna zaštita, metoda konačnih elemenata (FEM)*

Ahlem Chahinez Kadri: https://orcid.org/0009-0004-3703-923X
M'hamed Ouadah: https://orcid.org/0000-0003-3444-0787
Abderrahmane Younes: https://orcid.org/0000-0003-2446-1568
Sofiane Chabane: https://orcid.org/0000-0003-3720-1239